Model tests of gliding with different hindwing configurations in the four-winged dromaeosaurid *Microraptor gui*

David E. Alexander[a,1], Enpu Gong[b], Larry D. Martin[a,c], David A. Burnham[c], and Amanda R. Falk[c,d]

[a]Department of Ecology & Evolutionary Biology, University of Kansas, Lawrence, KS 66045-7534; [b]Department of Geology, Northeastern University, Shenyang, Liaoning 110004, China; [c]Division of Paleontology, Biodiversity Institute, University of Kansas, Lawrence, KS 66045-7561; and [d]Department of Geology, University of Kansas, Lawrence, KS 66045-7613

Edited by Alan Feduccia, University of North Carolina, Chapel Hill, NC, and accepted by the Editorial Board December 20, 2009 (received for review October 14, 2009)

Fossils of the remarkable dromaeosaurid *Microraptor gui* and relatives clearly show well-developed flight feathers on the hind limbs as well as the front limbs. No modern vertebrate has hind limbs functioning as independent, fully developed wings; so, lacking a living example, little agreement exists on the functional morphology or likely flight configuration of the hindwing. Using a detailed reconstruction based on the actual skeleton of one individual, cast in the round, we developed light-weight, three-dimensional physical models and performed glide tests with anatomically reasonable hindwing configurations. Models were tested with hindwings abducted and extended laterally, as well as with a previously described biplane configuration. Although the hip joint requires the hindwing to have at least 20° of negative dihedral (anhedral), all configurations were quite stable gliders. Glide angles ranged from 3° to 21° with a mean estimated equilibrium angle of 13.7°, giving a lift to drag ratio of 4.1:1 and a lift coefficient of 0.64. The abducted hindwing model's equilibrium glide speed corresponds to a glide speed in the living animal of 10.6 m·s^{-1}. Although the biplane model glided almost as well as the other models, it was structurally deficient and required an unlikely weight distribution (very heavy head) for stable gliding. Our model with laterally abducted hindwings represents a biologically and aerodynamically reasonable configuration for this four-winged gliding animal. *M. gui*'s feathered hindwings, although effective for gliding, would have seriously hampered terrestrial locomotion.

biomechanics | bird flight evolution | feathered dinosaurs | model tests | tetrapteryx

Evidence now exists that should settle the long-running debate over a ground-up origin of avian flight vs. the evolution of avian flight from a trees-down glider. This evidence shows that the protoavian was arboreal (1) rather than a terrestrial cursor as many have suggested (2–4). The leading protagonist in this controversy is presently a dromaeosaur, *Microraptor gui*, with a fully formed hind wing that is closely similar to its completely avian forewing (5), having elongate, aerodynamically advanced "primary feathers" coming off the metatarsi (5). There seems little reason to doubt the aerodynamic function of the hindwing, but there has been controversy over exactly how it was arranged and used for flight. We decided to address this problem by creating and testing models that closely replicate the anatomical features preserved in the now numerous fossils of *Microraptor* and its close relatives (discussed in *SI Text*).

Primitively, early archosaurs are sprawling, with the legs set laterally and elevated at around 75° (6), a preadapted posture for gliding. Modern birds normally have the thigh elevated and sprawled to the side in different degrees; for example, it is nearly perpendicular to the midline in loons and grebes (7). This variation shows that the degree of splaying needed to use the hindlegs in gliding is not unusual when compared with that in modern birds. The absence of an antitrochanter and a supracetabular shelf (SAC) in the eumaniraptorans, including dromaeosaurids, would make elevation and splaying of the legs even easier (8). Air pressure could have provided most of the force needed to elevate the leg into a gliding position similar to that in gliding mammals. This simple positioning was originally assumed for the four-winged *Microraptor gui* (5); but later, workers hoping to recover an upright posture proposed arrangements of the hindlimbs that would have required complicated systems of locks and muscles to hold the leg in an only partially elevated position, e.g., the "biplane" model (9). New anatomical information based on the discovery of several hundred specimens similar to the four-winged glider *M. gui* (and related taxa) has produced converging lines of evidence demonstrating that the original describers of *M. gui* (5) were correct in their interpretation of the flight posture. We postulate, based on examination of this new material, that *M. gui* was capable of abducting the hind limbs at least 65–70° to achieve a gliding posture.

We built a reconstruction of *Microraptor* (Fig. S1) based on bones cast in the round from LHV 0026, an articulated specimen (*SI Text*). This new specimen represents a larger individual and is probably a different species of *Microraptor* but is morphologically closely similar to *M. gui*, including the presence of flight-adapted feathers on the tarsometatarsus. We reconstructed the plumage using actual bird feathers trimmed to the correct size and shape, based mainly on the holotype of *M. gui* (IVPP V13352; Fig. S2 and Fig. S3) featured on the cover of *Nature* (2003, v. 421, no. 6921), as well as a survey of >100 additional specimens. We used the feathered reconstruction (Fig. S4) as a detailed pattern, along with airfoil shapes from modern birds, to build a molded urethane foam model (*SI Text*). We subjected the foam model to glide tests intended to determine whether our interpretation of the proportions and body plan of the extinct animal could have supported a gliding ecology during life. This model performed a number of successful glides, but it became apparent that we needed a more modular model with adjustable and replaceable components to allow us to analyze glide performance. This led us to design a model based on techniques used to build flying airplane models, which we refer to as the "flight model."

Author contributions: D.E.A., E.G., L.D.M., D.A.B., and A.R.F. designed research; D.E.A., E.G., L.D.M., D.A.B., and A.R.F. performed research; D.E.A. analyzed data; and D.E.A., L.D.M., and D.A.B. wrote the paper.

The authors declare no conflict of interest.

This article is a PNAS Direct Submission. A.F. is a guest editor invited by the Editorial Board.

See Commentary on page 2733.

[1]To whom correspondence should be addressed. E-mail: dalexander@ku.edu.

This article contains supporting information online at www.pnas.org/cgi/content/full/0911852107/DCSupplemental.

Results

We made glide tests on flight models with three different hindwing configurations: abducted (laterally elevated) with "cranked" or bent-up tips; abducted with straight tips; and the biplane configuration of Chatterjee and Templin (9) (*SI Text*). Both of the abducted hindwing configurations have an anhedral (negative dihedral) angle of 20° at the root (Fig. 1). We also used two different tail configurations. One tail had the tips of the surfaces angled up 20° forming a shallow V shape (the vee-tail) and one with the surfaces horizontal (the flat tail).

We analyzed six glides of the cranked-tip hindwing configuration launched from a height of 2.11 m, one of the same configuration from a launch height 3.33 m, and four of the straight-tip hindwing configuration from the 3.33 m launch height. Most flights were made with the vee tail. We also analyzed one flight with a flat tail (and the straight tip hindwing) and found no noticeable difference in stability relative to the vee-tail configuration.

Of the glides launched from a height of 2.11 m, 5 glides exceeded 17 m total length; the longest glide from this height, 19.1 m, yields a mean glide angle of 6.3°. Of the glides launched from a height of 3.33 m, four exceeded 22 m total length, including a glide of 23.9 m with a mean glide angle of 7.9°. These mean glide angles understate the actual equilibrium glide angles because they include level segments immediately after launching.

Glide angles measured from videos of the 11 glides analyzed ranged from 3° to 21°. Each glide was divided into equal early, middle, and late phases; because of the level segment right after the launch in the early phase, we ignored data from the early phase and focused on the middle and late phases. Fig. 2*A* shows that late in the glide, for both cranked tip and straight tip hind wings, the glide angles average 13–14°. Indeed, all but one of those glides had late glide angles of >11°. The angles in the middle of the glide are not as consistent, with the cranked tip configuration averaging only 70% of the straight-tip configuration's midglide angle. The glide angle, θ, defines the glide ratio, G (the distance flown forward for every unit distance of descent in altitude), by the relationship G = 1/(tan θ). In an equilibrium glide, the glide ratio is identical to the lift to drag ratio, L/D (10). The overall mean glide angle for all measured late glide segments was 13.7°. That glide angle yields G = 4.1. If we assume that this represents an equilibrium glide, it would indicate an L/D of 4.1.

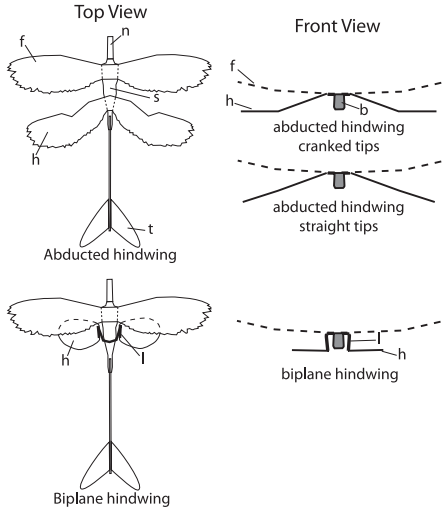

Fig. 1. Top and front views of the different configurations of the flight model. (*Top View*) Tracing showing the abducted hindwing and the biplane hindwing configurations. All components are the same except for the hindwings. (*Front View*) Schematic view showing the three hindwing configurations (dashed lines, forewings; solid lines, hindwings). Lengths, angles, and proportions are to scale. b, Polystyrene foam body; f, forewing; h, hindwing; l, aluminum wire leg skeleton (streamlined fairing omitted for clarity); n, neck plate for mounting balance weights; s, structural spine plate; t, tail.

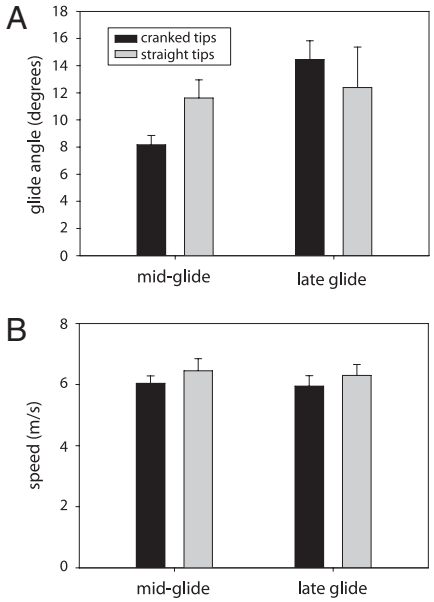

Fig. 2. (*A*) Average of glide angles measured in the middle third ("mid-glide") and last third ("late glide") of the videotaped glides. (*B*) Average of air speeds measured in the middle third and last third of the videotaped glides. Error bars show SE.

Although there was a slight variation in initial launch speeds (*SI Text*), the average glide speeds during the middle and late stages of the glide were very consistent, with averages of between 5.95 and 6.45 $m{\cdot}s^{-1}$ (Fig. 2*B*). The overall average glide speed from the middle and late glide segments was 6.14 $m{\cdot}s^{-1}$.

The biplane configuration had the main lifting surface of the hindwings extending 5 cm below the body (12 cm below the spine plate), so it could not be launched from our catapult. Thus, we chose to perform a hand launch of the biplane model at our indoor location, with a hand launch of the model in the straight-tip hindwing configuration ("abducted hindwing") for comparison. Both configurations were launched from a height of 4.43 m. Air speed of the abducted configuration immediately after launch was 7.54 $m{\cdot}s^{-1}$ and for the biplane was 7.66 $m{\cdot}s^{-1}$. Both models made substantial level flights before visibly pitching down into readily apparent descents. At 3.5 m into the level portion of the flight, the airspeed of both models was essentially the same, 6.65 $m{\cdot}s^{-1}$ for the abducted wing model vs. 6.67 $m{\cdot}s^{-1}$ for the biplane model. The level segment of the abducted hindwing model was 8.9 m long, and the speed at pitch-down was 4.7 $m{\cdot}s^{-1}$. The level segment of the biplane model was shorter (5.0 m), and it pitched down at a higher speed (6.65 $m{\cdot}s^{-1}$). Total glide length for the abducted hindwing model was 20.26 m vs. 18.03 m for the biplane model. The biplane model appeared to be in a near-equilibrium glide in the descending segment (with a very mild phugoid around a mean glide angle of 23°) because its air speed in the middle of the descent, 5.42 $m{\cdot}s^{-1}$, was essentially the same as its speed just before impact, 5.38 $m{\cdot}s^{-1}$. In contrast, the abducted hindwing model accelerated throughout the descending segment of the glide, with an air speed of 7.08 $m{\cdot}s^{-1}$ and a glide angle of 31° just before touchdown; it presumably would have leveled out eventually, given a great enough launch height. Although the touchdown speed of the biplane model was quite low (<5.5 $m{\cdot}s^{-1}$) compared with most glides of the other configurations, the location of the biplane hindwings caused them to impact first,

breaking the hindwings and preventing further glide tests of that configuration.

Comparing the two abducted configurations, the lower average glide angle for the cranked tip glides was most likely due to the fact that most of the measured glides for the cranked-tip configuration were launched from the lower height, so the middle of their glides were a bit earlier in time than the middle of the glides of most of the straight-tip configuration. The similarity in glide angles late in the glides suggests that the later stages of the glide were more likely to be in equilibrium.

Using the average wing area of the two abducted hindwings (0.143 m^2), and setting the average weight of those two configurations equal to lift (4.11 N), we can calculate the lift coefficient (C_L; *SI Text*). Based on our overall average glide speed of 6.14 $m{\cdot}s^{-1}$, we calculate $C_L = 0.640$.

Discussion

A positive dihedral angle is used by airplane designers to increase stability (11). Our *Microraptor* model's forewings had conventional positive dihedral (dihedral angle 2.4°, with additional 10° polyhedral at the tips), comparable to that used on model airplanes and by soaring birds. Its hip joint precludes *Microraptor* from having positive dihedral on the abducted hind wings, however, and limits them to having negative dihedral or anhedral. Even with the large anhedral angle (−20°) of the hind wings, the *Microraptor* model was surprisingly stable and gave reasonably straight glides in the majority of successful launches. We started our glide tests using the vee-tail configuration (essentially a small wing with dihedral of 20°) on the assumption that the stabilizing effect of such a tail might be necessary to counter the destabilizing effect of the hind wing. We chose the vee arrangement to augment stability, with the idea that the live animal might have had the feathers angled up into such a V-shape, or that flight loads might have passively bent them up. Although most modern birds fly with a flat tail fan, some birds, such as grackles, form the tail into a shallow V in slow flight. The shape of the tail surface corresponds to the shape of the fan of tail feathers in multiple fossils of *Microraptor* (Shandong Tianyo Museum of Natural History; *SI Text*). We also started with cranked tips on the hind wings, representing primary feathers free to bend upward a certain amount under flight loads, again to reduce the anhedral effect. We then tried hind wings with straight tips (representing stiffer feathers), which made no noticeable difference in stability. Finally, we tried a flat tail (dihedral = 0°). We analyzed one glide with the flat tail, which showed no apparent difference in stability from the glides with the vee tail. Thus, despite conventional airplane design principles, our model appeared to be quite stable, with a hind wing having substantial anhedral and a flat tail. Even the biplane configuration, which looked somewhat ungainly, proved to be quite stable once enough weight was added at the head to adjust the center of gravity to accommodate its more-forward hind wing location.

We discovered that the flight model was extremely sensitive in yaw to the head angle, which could provide a very simple, natural steering mechanism: "turn head to look left, turn left." The living animal probably could also perform some or all of the movements with its wings that are used by modern gliding birds. Whether the animal steered with its head or its wings, however, its stable configuration would have significantly reduced the control corrections needed to glide, which greatly simplifies the neural control requirements (12).

Although maximum steady-state lift coefficient values >1.0 have been reported for flying animals (13, 14), our model's glides were probably not performed at a high enough angle of attack to give the maximum lift coefficient. Our estimated equilibrium C_L value of 0.640 seems quite reasonable. It is within the range of values reported for large birds (15) and is actually quite close to the C_L value for minimum drag measured on a gliding hawk (16). In fact, a tandem-wing arrangement with a small anterior–posterior separation, as in our model, leads to some mutual interference such that less total lift is produced than would be produced by the sum of the front and hind wings operating separately. Given that we had limited ability to adjust the model's aerodynamic trim, and given the probable interference of the tandem configuration, a C_L value <1.0 is to be expected.

The overall average glide angle near the end of the measured glides was 13.7°. This corresponds to a L/D of 4.1. Although this is low compared with modern soaring birds of similar weight and wing area (e.g., red-tailed hawk: L/D = 10.0) (17), it is within the range for smaller birds such as budgerigars at 4.5 and crows at 5.0 (17) and wood ducks at 3.8 (13). Here again, the tandem-wing arrangement works against *Microraptor*: induced drag (i.e., drag caused by lift production) is a function of processes that occur mainly at the wing tip, and two tandem wings effectively have more tip than a single wing with the combined span and area of the tandem wings. This effect is related to the wing's aspect ratio, AR (AR = $[\text{span}]^2 \div$ planform area), where wings with higher AR have less induced drag. The forewings alone of our model have a very bird-like AR of 7.4, but when combined with the straight-tip hindwings, altogether the combined fore- and hindwings have an AR of only 3.7. By being two slightly separated wings instead of a single wing of aspect ratio 3.7, our model's fore- and hindwings will produce somewhat less induced drag than if they were really a single wing with an aspect ratio of 3.7 (short and broad), but more drag than a single wing with a span equal to the sum of the forewing and hindwing spans (long and narrow). Even treating them as a single wing, *Microraptor*'s aspect ratio is still substantially higher than the aspect ratios of 1.2–2.2 of such pure gliders as modern flying lizards (10), flying squirrels (18), and colugos (19), although some extinct reptilian gliders such as *Xianglong zhaoi* (20) had similar or even higher aspect ratios than those of *Microraptor*.

We can also compare our glide speeds with an engineering rule of thumb used to estimate flight speeds based on wing loading (17). Using the average weight and wing area of our two abducted hindwing models, this relationship gives a speed estimate of 6.2 $m{\cdot}s^{-1}$ (*SI Text*), essentially the same as our measured overall mean speed late in the glide of 6.1 $m{\cdot}s^{-1}$.

Our model's mass, 0.43 kg for the cranked-tip hindwings or 0.41 kg for the straight tip configuration, was much lower than the living *Microraptor*, because of our use of light-weight modeling materials. Based on water displacement tests with a detailed, anatomical reconstruction, we estimate that the live mass of a four-winged *Microraptor* specimen the size of our model would have been 1.23 kg, giving a weight of 12.1 N. Using the same wing geometry as our model and the weight of a live animal, Tennekes's rule of thumb yields a glide speed estimate of 10.6 $m{\cdot}s^{-1}$. Modern birds with similar weight and wing area include the common buzzard (weight (W) = 10.0 N, wing area (S) = 0.27 m^2, estimated flight speed (v) = 9.9 $m{\cdot}s^{-1}$), the red-tailed hawk (W = 10.9 N, S = 0.209 m^2, v = 11.7 $m{\cdot}s^{-1}$), and the roseate spoonbill (W = 13 N, S = 0.226 m^2, v = 12.3 $m{\cdot}s^{-1}$) (17). Although *Microraptor* would have had a flight speed similar to the flight speeds of these birds, the hawks have L/D values of ~10.0 (10), which means that they would have a much flatter equilibrium glide than that of *Microraptor*.

The model in the biplane configuration proposed by Chatterjee and Templin (9) could be made to glide reasonably well, although probably with a steeper equilibrium glide than our abducted hindwing configurations; but our model tests revealed some problems with this concept. Because of the hindlimb posture, the biplane hindwings only provided 0.049 m^2 of wing area, as opposed to >0.14 m^2 for either of the abducted hindwings. Thus, the total wing area of the biplane configuration is only two thirds of the area of the other configurations. Moreover, this configuration was heavier: even though its hindwings were lighter, the forward location of the hindwings required the center of gravity (CG) to be located 9.5 cm anterior to the CG location

of the other configurations. This required adding >200 g of weights to the head region of the biplane configuration, as opposed to the 50–60 g needed to position the CG of the other configurations. Thus, the total weight of the biplane configuration corresponded to a live weight of 13 N, which, combined with the lower wing area, gave it a wing loading 78% higher than the other configurations. This wing loading produces a flight speed estimate of 13.4 $m \cdot s^{-1}$.

The weight needed in the head region to properly position the CG in the biplane configuration suggests that this was not a practical posture for the live animal. A mass of 200 g for the head of the model corresponds to a head mass of 500 g in the live animal. Given a head volume of ≈105 cm^3, such a head weight seems physically impossible and, indeed, would represent more than one third of the estimated live mass of the whole animal. In contrast, the weight needed to balance the models with abducted hindwings implies a 125–150-g head mass, which is an excellent match with the likely head volume (being a mixture of bone with a density of 2 g/cm^3 and soft tissue at ≤1 g/cm^3).

In addition, in the biplane configuration, the feathers on the hind limb proximal to the ankle could not be used for lift production, only for streamlining the leg. Yet the length and vane asymmetry of these feathers are classic indicators of lift-producing flight feathers (21, 22). Finally, our model tests demonstrated that the abducted configuration of the hindwing is much less fragile and better positioned to support flight and landing loads than the biplane configuration. In the biplane configuration, flight forces must be resisted actively by muscles, and the bones are not oriented to carry vertical loads efficiently. In the abducted hindwing configurations, natural limits on articulations allow much of the aerodynamic load to be carried passively, and the forces are spread out along the length of the wing, making the bones' orientation more mechanically efficient.

Almost a century ago, William Beebe suggested that modern birds might have a four-winged ancestor, and he presented a hypothetical description strikingly similar to our flight models of *Microraptor* (23). Our flight model of a four-winged *Microraptor* in the configuration with abducted hindwings is entirely consistent with the fossil evidence, including recent observation of many new fossil specimens of *Microraptor* and related animals (*SI Text*) (24). Our physical model proved to be a surprisingly stable passive glider with aerodynamic characteristics within the range of modern birds. Indeed, a tandem wing arrangement is considered less sensitive to center of gravity variations and hence is inherently more longitudinally stable (25). Obviously, the living animal was capable of active control, but we suggest that the tandem wing configuration may have been advantageous because it requires less active stabilizing ability. It would thus have less need of the reflexes associated with active stabilization as used by modern powered flying animals (11), although possibly at the expense of some maneuverability. We suggest that *Microraptor* was an adept glider and would have had little difficulty gliding from tree trunk to tree trunk or climbing trees, but would have been very awkward and vulnerable on the ground. The primary feathers on the tarsometatarsus (foot) of the hindwing of *M. gui* were too long in relation to the limb bones to have allowed the hindwing to fold compactly as does the modern bird wing. Just as colugos and sloths have their limbs encumbered by patagia, the hindwing feathers on *Microraptor* would severely hamper any terrestrial locomotion.

Materials and Methods

Glider Design. We used the urethane foam model, patterned after the feathered model, for numerous hand-launched glides, but it was not robust enough for catapult launching and it allowed no reasonable way to test different configurations. Thus, we designed a flight model based on techniques used to build flying airplane models. The wings were a combination of plastic film–covered, balsa rib-and-spar framework and thin, curved balsa sheets, carefully matched to the shape of the feathered model. A thin plywood plate on top of a polystyrene foam body defined the zero-incidence plane and supported the wings, tail, and neck plate (for adding weights at the head location to adjust the center of gravity). All models used the same forewings, set in a typical gliding bird posture with slight dihedral. We built three hindwings, two abducted laterally and angled down 20° from the horizontal (representing 65–70° of abduction): one with tips "cranked" or bent up to be horizontal; one with tips aligned with the rest of the wing; and one in the biplane posture of Chatterjee and Templin (9). The biplane hindwing was essentially a wire skeleton holding the wing tip below the belly of the body and abducted laterally (Fig. S4 and Fig. S5). The tail, a carbon-fiber tube with balsa plates representing plumage, was attached to the body via a joint that could be adjusted between glides to increase or decrease the tail incidence. Most glides used a tail with tips of the plumage elevated into a shallow V shape, but a tail with flat plumage was also used (construction details and dimensions in *SI Text*).

The balsa–plywood–foam flight model is intended to be a 1:1 scale model of the fossil specimen. Dimensions are given in Table S1, and the various configurations are shown in Fig. 1, Fig. S6, and Fig. S7.

To provide stability, gliding airplane models typically have ballast weights added to place the craft's center of gravity (CG) at or near 25% of the wing's mean chord length aft of the wing's leading edge—the "quarter-chord" location (26)—which places the CG at the wing's aerodynamic center (AC) (27). For tandem-winged craft, the AC will be between the two wings (*SI Text*). We added lead weights to the front of the body and to the neck platform at the location of the head to place the CG of the two abducted hindwing configurations 12.2 cm behind the forewing root leading edge. Because the biplane hindwings are much smaller than the abducted hindwings, and the biplane hindwings are so far forward they partly overlap the forewings, the CG of the biplane configuration was 2.7 cm behind the forewing root leading edge.

Catapult Launcher. Glide tests of the molded-foam model and the first configuration of the flight model demonstrated that launching by hand was too inconsistent to achieve a repeatable performance. We thus built a launcher that accelerated the model to flight speed using a stretched length of latex rubber surgical tubing. When properly set up, the catapult launched the model at well above the model's stall speed.

Glide Tests. Hand-launching the molded-foam model in outdoor locations demonstrated the need for a more controlled setting, so all glide tests of the balsa–plywood–foam flight models were made indoors, on an indoor football practice field, with the launcher mounted on a pair of step ladders. A tripod-mounted digital camcorder recorded glides. Videos were played back frame-by-frame on Macintosh computers using iMovie software and analyzed by hand (*SI Text*). Angles were measured directly, and displacements and known time intervals between frames were used to calculate speeds.

ACKNOWLEDGMENTS. We thank the Liaoning Province Department of Land and Resources for loaning us fossils, and we thank the Institute of Vertebrate Paleontolgy and Paleoanthropology, Beijing, China, the Dalian Natural History Museum, and the Shandong Tianyu Museum of Natural History for access to specimens and their generous hospitality during our visits. We also thank Richard Bramlette for helping with aerodynamic calculations; Richard Colgren for helping design one of the hindwing models and access to the Aerospace Engineering Department's Vehicle Manufacturing Facility; Richard Colgren and Ron Barrett-Gonzalez for helpful discussions about the characteristics of different wing configurations; John Chorn, David Biller, and Michael Lemmon for x-rays of fossils; and Jay Ellis for access to Anschutz Sports Pavillion. Charles Hines helped design the wings of the foam model, Allan Hemmy helped design and build the catapult, Kenneth Bader helped construct the feathered model and Tom Swearingen sculpted the body and provided feathers. Kevin Alexander, Richard Bramlette, TJ Meehan, Ali Nabavizadeh, Suman Sadhu, and Jack Swab provided valuable assistance with glide tests; Greg Ornay and Taylor Lenon filmed glides at both sites; and Greg Ornay and Ali Nabavizadeh helped with video formatting and file transfers. The authors thank Duane Robinson for technical support on Utah Foam Products, and staff at George's Hobby Shop, Lawrence, KS, for providing helpful conversations on model construction. This investigation was supported by the University of Kansas General Research Fund and Center for East Asian Studies.

1. Norberg UM (1985) Evolution of vertebrate flight: An aerodynamic model for the transition from gliding to active flight. *Am Nat* 126:303–327.

2. Padian K, Chiappe LM (1998) The origin and early evolution of birds. *Biol Rev Camb Philos Soc* 71:1–42.

3. Burgers P, Chiappe LM (1999) The wing of *Archaeopteryx* as a primary thrust generator. *Nature* 399:60–62.
4. Ostrom JH (1974) *Archaeopteryx* and the origin of flight. *Q Rev Biol* 49:27–47.
5. Xu X, et al. (2003) Four-winged dinosaurs from China. *Nature* 421:335–340.
6. Bakker RT (1971) Dinosaur physiology and the origin of mammals. *Evolution* 25: 636–658.
7. Hertel F, Campbell KE, Jr. (2007) The antitrochanter of birds: Form and function in balance. *Auk* 124:789–805.
8. Longrich N (2006) Structure and function of hindlimb feathers in *Archaeopteryx lithographica. Paleobiology* 32:417–431.
9. Chatterjee S, Templin RJ (2007) Biplane wing planform and flight performance of the feathered dinosaur *Microraptor gui. Proc Natl Acad Sci USA* 104:1576–1580.
10. Alexander DE (2002) *Nature's Flyers: Birds, Insects, and the Biomechanics of Flight* (Johns Hopkins University Press, Baltimore), pp 358.
11. Alexander DE (2009) *Why Don't Jumbo Jets Flap Their Wings? Flying Animals, Flying Machines, and How They Are Different* (Rugters University Press, New Brunswick, NJ), pp 278.
12. Maynard Smith J (1952) The importance of the nervous system in the evolution of animal flight. *Evolution* 6:127–129.
13. Withers PC (1981) An aerodynamic analysis of bird wings as fixed aerofoils. *J Exp Biol* 90:143–162.
14. Tucker VA (1988) Gliding birds: Descending flight of the white-backed vulture *Gyps africanus. J Exp Biol* 140:325–344.
15. Pennycuick CJ, Heine CE, Kirkpatrick SJ, Fuller MR (1992) The profile drag of a hawk's wing measured by wake sampling in a wind tunnel. *J Exp Biol* 165:1–19.
16. Tucker VA, Heine C (1990) Aerodynamics of gliding flight in a Harris' hawk *Parabuteo unicinctus*. *J Exp Biol* 149:469–490.
17. Tennekes H (1996) *The Simple Science of Flight: From Insects to Jumbo Jets* (MIT Press, Cambridge, MA), pp 137.
18. Thorington RW, Jr, Heaney LR (1981) Body proportions and gliding adaptations of flying squirrels (Petauristinae). *J Mammal* 62:101–114.
19. Stafford BJ (1999) Taxonomy and Ecological Morphology of the Flying Lemurs (Dermoptera, Cynocephalidae). Ph.D. dissertation (City University of New York, New York).
20. Li P-P, Gao K-Q, Hou L-H, Xu X (2007) A gliding lizard from the Early Cretaceous of China. *Proc Natl Acad Sci USA* 104:5507–5509.
21. Norberg RÅ (1985) Function of vane asymmetry and shaft curvature in bird flight feathers; inferences on flight ability of *Archaeopteryx. The Beginnings of Birds,* Proceedings of the International *Archaeopteryx* Conference, Eichstätt, 1984, eds Heckt MK, Ostrom JH, Viohl G, Wellnhofer P (Freunde des Jura-Museums Eichstätt, Eichstätt, Germany), pp 303–318.
22. Feduccia A, Tordoff HB (1979) Feathers of *Archaeopteryx*—asymmetric vanes indicate aerodynamic function. *Science* 203:1021–1022.
23. Beebe CW (1915) A tetrapteryx stage in the ancestry of birds. *Zoologica* 2:38–52.
24. Hu D, Hou L, Zhang L, Xu X (2009) A pre-*Archaeopteryx* troodontid theropod from China with long feathers on the metatarsus. *Nature* 461:640–643.
25. Poulsen CM (1943) The tandem monoplane: Does it still have a future? Some past experiences recalled. *Flight Int* 44 (1807):167–168.
26. Simons M (1987) *Model Aircraft Aerodynamics* (Argus Books, Hemel Hempstead, Hertfordshire, United Kingdom.), pp 318.
27. Bertin JJ, Smith ML (1979) *Aerodynamics for Engineers* (Prentice-Hall, Englewood Cliffs, NJ), pp 410.